

Original Article

Combined effects of a high-fat diet and chronic valproic acid treatment on hepatic steatosis and hepatotoxicity in rats

Li-fang ZHANG^{1, #}, Ling-sheng LIU^{1, #}, Xiao-man CHU², Hao XIE¹, Li-juan CAO¹, Cen GUO¹, Ji-ye A¹, Bei CAO¹, Meng-jie LI¹, Guang-ji WANG^{1, *}, Hai-ping HAO^{1, *}

¹State Key Laboratory of Natural Medicines, Key Laboratory of Drug Metabolism and Pharmacokinetics, China Pharmaceutical University, Nanjing 210009, China; ²Department of Clinical Pharmacology, Jinling Hospital, Nanjing 210002, China

Aim: To investigate the potential interactive effects of a high-fat diet (HFD) and valproic acid (VPA) on hepatic steatosis and hepatotoxicity in rats.

Methods: Male SD rats were orally administered VPA (100 or 500 mg·kg⁻¹·d⁻¹) combined with HFD or a standard diet for 8 weeks. Blood and liver samples were analyzed to determine lipid levels and hepatic function biomarkers using commercial kit assays. Low-molecular-weight compounds in serum, urine and bile samples were analyzed using a metabonomic approach based on GC/TOF-MS.

Results: HFD alone induced extensive hepatocyte steatosis and edema in rats, while VPA alone did not cause significant liver lesions. VPA significantly aggravated HFD-induced accumulation of liver lipids, and caused additional spotty or piecemeal necrosis, accompanied by moderate infiltration of inflammatory cells in the liver. Metabonomic analysis of serum, urine and bile samples revealed that HFD significantly increased the levels of amino acids, free fatty acids (FFAs) and 3-hydroxy-butanoic acid, whereas VPA markedly decreased the levels of amino acids, FFAs and the intermediate products of the tricarboxylic acid cycle (TCA) compared with the control group. HFD aggravated VPA-induced inhibition on lipid and amino acid metabolism.

Conclusion: HFD magnifies VPA-induced impairment of mitochondrial β -oxidation of FFAs and TCA, thereby increases hepatic steatosis and hepatotoxicity. The results suggest the patients receiving VPA treatment should be advised to avoid eating HFD.

Keywords: valproic acid; high-fat diet; drug diet interaction; non-alcoholic fatty liver disease; hepatotoxicity; tricarboxylic acid cycle; amino acid; free fatty acid; metabonomics

Acta Pharmacologica Sinica (2014) 35: 363–372; doi: 10.1038/aps.2013.135; published online 20 Jan 2014

Introduction

Valproic acid (2-propyl-pentanoic acid, VPA) is an 8-carbon branched-chain fatty acid that has been a first-line therapy in the treatment of epilepsy for more than 30 years^[1, 2]. More recently, studies have found that VPA is a potential anti-cancer agent, due in part to its anti-histone deacetylase activity^[3, 4]. VPA has broad applications. For this reason, the side effects associated with VPA, especially hepatotoxicity, have aroused widespread global concern^[5, 6]. Abdominal ultrasound studies showed the presence of non-alcoholic fatty liver disease (NAFLD) in 61% of VPA-treated patients^[7], which suggested a high frequency of changes in asymptomatic hepatic steatosis

induced by VPA.

Until now, the mechanisms underlying the hepatotoxicity of VPA have remained unclear and actively debated. However, the impairment of hepatic mitochondrial function is widely thought to be important^[8, 9]. In addition, pre-existing mitochondrial impairment could increase hepatic vulnerability to VPA toxicity^[10, 11]. These observations prompted us to hypothesize that VPA may combine with other etiological factors with the net consequence of increasing the frequency and severity of liver injury.

Food preferences contribute to the physiological diversity among individuals, especially in patients, because food may influence metabolic patterns and the efficacy of drugs^[12, 13]. It is well known that a high-fat diet (HFD) is a major contributing factor in the prevalence of NAFLD, which is defined as the significant accumulation of fat in the liver (>5%–10% of the weight of the liver), which can be as high as 76% in obese subjects^[14–16]. Because of changes in lifestyles, the prevalence

These authors contributed equally to this work.

* To whom correspondence should be addressed.

E-mail hhp_770505@yahoo.com.cn (Hai-ping HAO);

guangjiwang@hotmail.com (Guang-ji WANG)

Received 2013-06-01 Accepted 2013-08-23

of NAFLD in developing countries has increased rapidly over the past decade and has now reached levels close to those seen in Western countries (approximately 30% of the general population)^[17]. Although most patients diagnosed with NAFLD are asymptomatic, the liver becomes quite vulnerable when challenged by other stressors such as alcohol and drugs^[18]. Accumulating evidence suggests that mitochondrial dysfunction is involved in the early pathological manifestations of NAFLD^[19, 20]. As discussed above, long-term treatment with VPA is associated with mitochondrial impairment and represents a risk factor for the development of NAFLD^[21]. Because both VPA and an HFD can induce mitochondrial impairment in hepatocytes, it is very likely that both factors can amplify each other and subsequently increase the risk and extent of liver injury. Considering the high prevalence of NAFLD and the wide application of VPA, it is highly likely that both factors exist concurrently in clinical patients, and thus, their interactive effect should be of major concern.

Metabolomics is defined as “the quantitative measurement of metabolic responses to physiological and pathological stimuli”^[22]; it can provide a holistic evaluation of the low-molecular-weight compounds found in biofluids, cells, tissues, and organisms. Metabolomics has been widely applied to monitor metabolic modifications, pathophysiological changes, or the exogenous challenges caused by disease, drugs, toxicants, and genetic changes^[23, 24]. Hepatic injuries induced by both VPA and HFD are characterized by mitochondrial dysfunction. A metabolomic approach would be expected to provide direct and detailed insights about pathological development and the mechanisms involved in disease processes. In addition, some metabolomic studies have assessed the hepatotoxicity induced by VPA or metabolic disorders associated with NAFLD^[25, 26]. However, very little is known about the possible interactions between chronic VPA treatment and HFD with regard to the induction of hepatic steatosis and hepatotoxicity.

In this study, VPA combined with an HFD was administered to Sprague-Dawley rats to induce NAFLD. The endogenous metabolite levels in serum, bile and urine were profiled using a gas chromatography/time-of-flight mass spectrometry (GC/TOF-MS)-based metabolomics platform. We aimed to clarify the effects of chronic VPA treatment and an HFD on metabolic pathways involved in hepatic steatosis and hepatotoxicity.

Materials and methods

Chemicals and reagents

Valproate sodium (VPA-Na, purity 99%) was obtained from Zelang Medical Technology (Nanjing, China). (¹³C)₂-Myristic acid, 99 atom % ¹³C (IS) was obtained from Sigma-Aldrich (St Louis, MO, USA). Alkane series (C₈-C₄₀), MSTFA (*N*-methyl-*N*-trimethylsilyltrifluoroacetamid) plus 1% TMCS (trimethylchlorosilane), and pyridine (silylation grade) were obtained from Pierce Chemical (Rockford, USA). HPLC-grade (>99.5%) methanol and *n*-heptane were obtained from Tedia (Fairfield, USA). All the other reference compounds were obtained from Sigma-Aldrich, Merck (Darmstadt, Germany), or Serva (Hei-

delberg, Germany). Purified water was produced by a Milli-Q system (Millipore, MA, USA). Stock solutions of the reference compounds and IS were prepared either in purified water or methanol.

Animals and treatments

Male Sprague-Dawley rats (with a mean weight of 200–220 g) were obtained from Slac Inc (Shanghai, China), caged and fed under standard environmental conditions (20–25 °C with a 12-h light-dark cycle and free access to food and water). All the animal experimental procedures were approved by the local Animal Care and Use Committee of the China Pharmaceutical University and designed in accordance with the guiding principles for the use of animals in toxicology adopted by the Chinese Society of Toxicology. The standard diet followed the national standard (GB 14924.3-2010, China), and the HFD was 77.5% *w/w* standard diet plus 10% *w/w* protein, 10% *w/w* coconut oil, 2% *w/w* cholesterol, and 0.5% *w/w* bile salt. VPA-Na was dissolved in distilled water. The animals were acclimatized to the facilities and fed an initial corn starch-based diet for 1 week. The animals were then randomly assigned to 1 of 6 groups with 6 rats in each group: the control group (standard diet), the model group (HFD), the V100 group (VPA-Na, 100 mg·kg⁻¹·d⁻¹, ig), the V500 group (VPA-Na, 500 mg·kg⁻¹·d⁻¹, ig), the MV100 group (VPA-Na, 100 mg·kg⁻¹·d⁻¹, ig and HFD), and the MV500 group (VPA-Na, 500 mg·kg⁻¹·d⁻¹, ig and HFD). All the rats were raised for 8 consecutive weeks. The duration of the experiment was based on two major factors: 1) VPA-induced microvesicular steatosis was developed in the early weeks of therapy, and 2) the rats treated with an HFD for 8 weeks showed initial evidence of NAFLD^[5, 27]. Two dose levels of VPA, a therapeutic level (100 mg/kg) and a subtoxic level (500 mg/kg), were selected^[28, 29]. All the animals were weighed and observed every day to confirm the ingestion of the provided diet, evidence of any abnormal clinical conditions, or mortalities. At the conclusion of the experiment, all the rats were transferred to metabolism study cages and allowed to acclimatize for 2 d. Urine samples were then collected for 24 h in 50 mL polypropylene tubes containing 0.2 mL of 2% sodium azide, and the urine volumes were measured and recorded. In addition, 1-mL blood samples were collected. The blood and urine samples were immediately stored at -70 °C before measuring the analytes. The next morning, all the rats had a bile duct cannulation under anesthesia following reported techniques with minor adjustments^[30, 31], and bile was collected for 4 h. After this procedure, all the animals were euthanized, and the liver tissues were promptly removed and weighed and immediately frozen in liquid nitrogen until use.

Biochemical and histopathological analysis

Levels of triglycerides (TG), total cholesterol (TC), free fatty acids (FFAs), high-density lipoproteins (HDL), low-density lipoproteins (LDL), alanine aminotransferase (ALT), aminotransferase (AST), malondialdehyde (MDA), glutathione S-transferase (α-GST) in rat plasma, and TG, TC, and FFAs in

the liver were measured with an automatic blood biochemical analyzer (Beckman Counter LX20, USA). Sections of the same part of the livers were dissected, fixed in a phosphate-buffered 10% formaldehyde solution and then embedded in paraffin wax. Sections of liver were also stained with hematoxylin and eosin (H&E) and examined for histopathological changes by an experienced pathologist using light microscopy (Olympus BH2, Japan).

Preparation of samples

Serum, urine, and bile samples were processed, extracted, and derived in accordance with our previously developed methods^[32-34]. Briefly, the specimens were thawed by incubating them at 37 °C for 20 min and centrifuged at 1600×g for 10 min at 4 °C. For urine samples, an equal volume of urease (20 IU) solution was added to 50 µL of urine; the mixtures were then incubated at 37 °C for 1 h to decompose the excess urea. Next, 50 µL of the mixture were prepared as described above for serum and as described below for bile. Two hundred microliters of methanol containing the internal standard (¹³C₂)-myristic acid (12.5 µg/mL for serum and bile and 27.5 µg/mL for urine) were added to the specimens (50 µL). The specimens were vigorously extracted for 3 min and centrifuged at 20000×g for 10 min at 4 °C. Next, 100 µL of the supernatant were transferred and evaporated in a vacuum (Savant Instruments, Framingham, NY, USA); 30 µL ethoxyamine in pyridine (10 mg/mL) were then added to the desiccated residue, and the mixture was vigorously vortex-mixed for 2 min. The methoximation reaction was performed for 16 h at room temperature, followed by trimethylsilylation for 1 h, which was completed by adding 30 µL of MSTFA with 1% TMCS as the catalyst. Finally, the specimens were vortex-mixed again for 30 s following the addition of the external standard methyl myristate in heptane (30 µg/mL), which was transferred to a GC vial for the GC/TOF-MS analysis.

GC/TOF-MS analysis

To diminish the opportunity for systematic variation, all the samples were randomly selected for analysis by GC/TOF-MS. A 1-µL portion of the derived samples was injected into an Agilent 6890N GC system (Agilent Technologies, Atlanta, GA, USA) with an Agilent 7683 auto-sampler and analyzed by Pegasus III MS (Leco Corp, St Joseph, MI, USA) as we have described previously^[35]. To achieve good separation, the column temperature was initially kept at 80 °C for 2 min, increased from 80 to 200 °C at 25 °C/min, held for 0.5 min, increased from 200 to 300 °C at 35 °C/min, and held for 1 min. The mass spectra were acquired over the mass range of 50–700 *m/z* at a rate of 25 spectra/s after a solvent delay of 160 s. Automatic peak detection and mass spectrum deconvolution were performed with ChromaTOF™ software (Leco, version 3.25) as reported previously^[36].

Identification of endogenous metabolites

Each of the detected endogenous compounds was identified by comparing the mass spectrum and retention indexes for the

analyte with authentic reference standards or those available in various libraries [eg, Mainlib and Publib in the National Institute of Standards and Technology (NIST) library 2.0 (2008) and Wiley 9 (Wiley-VCH Verlag GmbH & Co KGaA, Weinheim, Germany)].

Multivariate data analysis and statistics

For the serum and bile data, the acquired peak areas were normalized against the IS values; for the urinary data, the peak areas were normalized according to the urine volume of each animal. The normalized data were then exported into Soft Independent Modeling of Class Analogy software (SIMCA)-P (version 11.0, Umetrics AB, Umea, Sweden). Unit variance scaling was used, and the data were evaluated in SIMCA-P 11 software for multivariate statistical measures^[37-39]. A principal component analysis (PCA) and a partial least squares projection to latent structures and discriminant analysis (PLS-DA) were then used to process these data. The statistical analysis of the differences between the groups with regard to biochemical parameters or metabolites was performed using one-way analyses of variance (ANOVA) with a significance level of *P*<0.05 or 0.01. The statistical analyses were performed using SPSS software version 16.0 (SPSS, Chicago, USA).

Results

Liver histopathology

Liver histopathology was evaluated by performing a gross histological and microscopic examination. Neither low-dose (100 mg·kg⁻¹·d⁻¹) nor high-dose (500 mg·kg⁻¹·d⁻¹) VPA alone caused significant changes in morphologically evident liver lesions, with the notable exception of infrequent hepatocyte steatosis in the rats in the V500 group. HFD alone induced extensive hepatocyte steatosis and edema. Co-treatment with VPA and HFD induced additional spotty or piecemeal necrosis, predominantly located in both the periportal and pericentral zones of the liver, compared with the model group. These histological changes were accompanied by moderate infiltration with inflammatory cells (Figure 1).

Biochemical analysis

As we have reported previously^[40], the plasma and liver levels of all lipids (with the exception of HDL) were significantly higher in the HFD-treated groups compared with those in the control group. Notably, the plasma levels of TC, LDL, and HDL were significantly reduced in the VPA mono-treatment groups, whereas the levels of both TG and FFAs increased in the V500 group. However, the liver levels of TC, TG, and FFAs were significantly higher in the co-treatment groups than in the HFD or VPA mono-treated groups. This indicated that VPA and HFD further aggravated the accumulation of liver lipids.

Typical serum biomarkers of hepatic function, including ALT, AST, MDA, and α-GST, were determined. The levels of all serum biomarkers (with the exception of α-GST) were significantly increased after the HFD was consumed for 8 weeks compared with the normal control diet, indicating serious

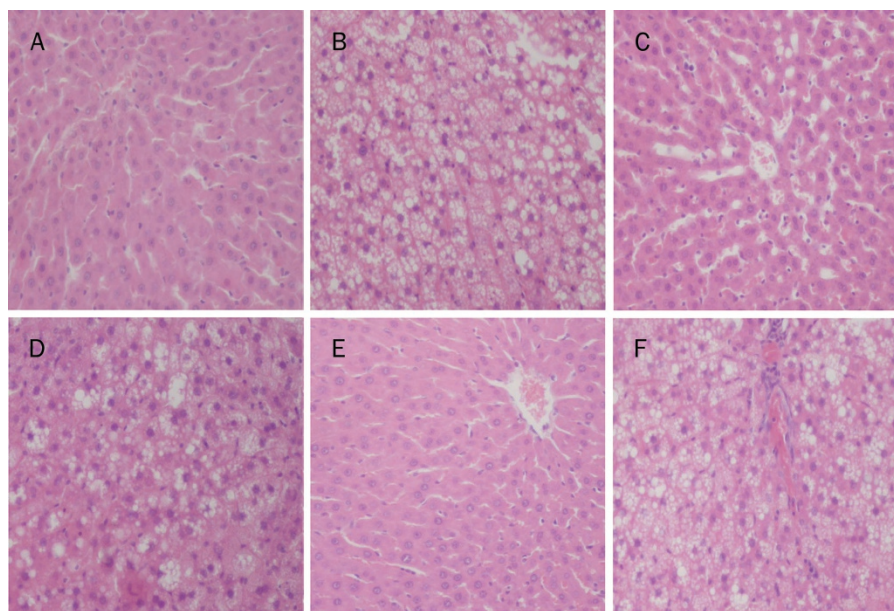


Figure 1. Histopathological assessment of rats following 8 weeks of treatment. (A) Control group (rats receiving only a standard diet); (B) Model group (rats receiving only an HFD); (C) V100 group (VPA, 100 mg·kg⁻¹·d⁻¹, ig, and a standard diet); (D) MV100 group (VPA, 100 mg·kg⁻¹·d⁻¹, ig, and an HFD); (E) V500 group (VPA, 500 mg·kg⁻¹·d⁻¹, ig, and a standard diet); (F) MV500 group (VPA, 500 mg·kg⁻¹·d⁻¹, ig, and an HFD).

hepatic injury. The rats treated with VPA also showed the same trends as those fed an HFD. However, only MDA and α -GST demonstrated statistically significant changes in the V100 and V500 groups. Additionally, an HFD combined with VPA further aggravated the abnormalities in these hepatic function biomarkers.

Metabonomic analysis of serum, urine, and bile samples

The metabonomic analysis of serum, urine, and bile samples was performed in accordance with our previously described GC/TOF-MS approach^[35, 36]. Representative chromatograms of the total ion current (TIC) of the various groups are shown in Supplementary Table S1 and Figure S1–S3. A visual inspection of the chromatograms revealed some differences between the groups. After the deconvolution of these profiles, 78 of 237 peaks for the bile samples, 98 of 204 peaks for the serum samples, and 88 of 206 peaks for the urine samples were identified and semi-quantified. For the bile, serum, and urine samples, the relative standard deviations of the internal standards were 9.44%, 7.28%, and 3.65%, respectively, and the external standards were 4.63%, 10.25%, and 10.70%, respectively. These data supported the high reproducibility of the sample preparation process and the stability of the analytical system.

Metabolic patterns based on the analysis of the bile data

Changes in metabolic patterns can be more accurately depicted with local biofluids than with systemic biofluids such as serum or urine. Bile immediately and directly reflects the pathological changes in the liver more than other biofluids such as serum or urine. A two-component PCA model ($R^2X=0.429$, $Q^2Y=0.287$, Figure 2) showed that each group of

samples clustered closely. The PLS-DA model ($R^2X=0.492$, $R^2Y=0.491$, and $Q^2Y=0.286$, Figure 3) showed the same general distribution. All the rats treated with an HFD (model, MV100, and MV500 groups) were located in the lower part of the figure relative to the controls (control, V100, and V500 groups). By contrast, the rats treated with VPA (V100, V500, MV100, and MV500 groups) clustered to the left side relative to their controls (control and model groups). The combined effects of HFD and VPA were clearly demonstrated in the scoring plot, and their clustering on the lower left indicated the combined influence of the HFD (drifting to the left side) and VPA (drifting to the lower quadrants of the plot).

Metabolic patterns based on the analysis of the urine data

An unsupervised analysis of the PCA model of urinary data (three components, $R^2X=0.625$, $Q^2Y=0.432$) revealed an outlier in the MV100 group (Figure 2). The outlier had marked chemical differences from the other samples in MV100. The PCA scoring plot for the urinary samples showed that the discrimination between low-dosage VPA groups (V100 and MV100) and high-dosage VPA groups (V500 and MV500) was poor. To achieve better discrimination, we generated a three-component PLS-DA model that explained and predicted 94.3% and 84.5% of the variation in the samples, respectively. The R^2X , R^2Y , and Q^2Y parameters were 0.605, 0.943, and 0.845, respectively (Figure 3). In general, the urine samples showed similar clustering to the bile samples. The HFD tended to shift the plots toward the left side, and intervention with VPA tended to shift the plots towards the lower left side. The combined effects of HFD and VPA resulted in further clustering to the left. The scoring plot showed distinct dose-dependent varia-

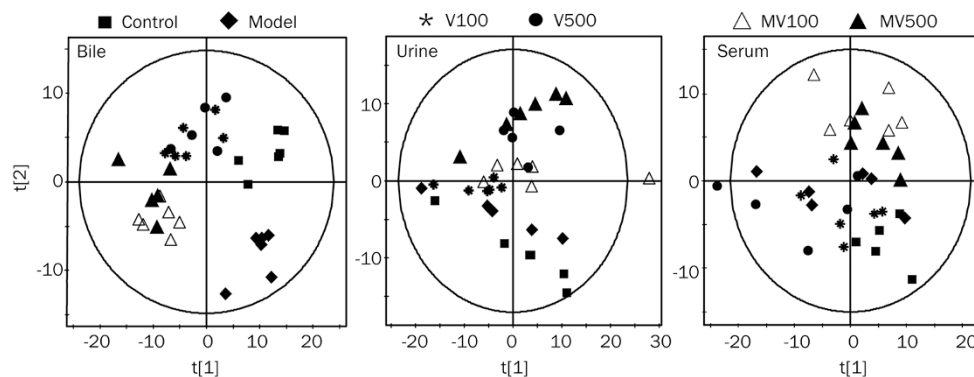


Figure 2. PCA scoring plots for analyzing GC/TOF-MS data collected from assessing rat serum, urine, and bile. ■, Control group (rats receiving only a standard diet); ◆, Model group (rats receiving only an HFD); *, V100 group (VPA, 100 mg·kg⁻¹·d⁻¹, ig, and a standard diet); ●, V500 group (VPA, 500 mg·kg⁻¹·d⁻¹, ig, and a standard diet); △, MV100 group (VPA, 100 mg·kg⁻¹·d⁻¹, ig, and an HFD); ▲, MV500 group (VPA, 500 mg·kg⁻¹·d⁻¹, ig, and an HFD).

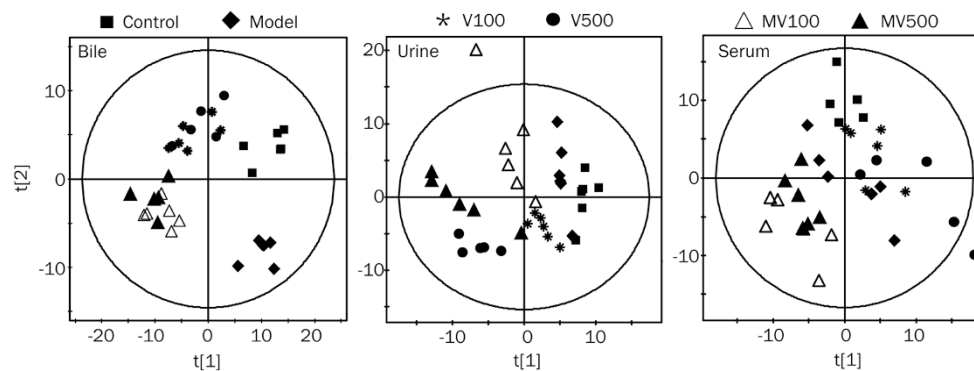


Figure 3. PLS-DA scoring plots for analyzing GC/TOF-MS data collected from assessing rat serum, urine, and bile. ■, Control group (rats receiving only a standard diet); ◆, Model group (rats receiving only an HFD); *, V100 group (VPA, 100 mg·kg⁻¹·d⁻¹, ig, and a standard diet); ●, V500 group (VPA, 500 mg·kg⁻¹·d⁻¹, ig, and a standard diet); △, MV100 group (VPA, 100 mg·kg⁻¹·d⁻¹, ig, and an HFD); ▲, MV500 group (VPA, 500 mg·kg⁻¹·d⁻¹, ig, and an HFD).

tions both for VPA mono-treatments (V100 and V500) and the combined treatments (MV100 and MV500).

Metabolic patterns based on the serological data

The PCA scoring plot for the serum samples suggested that the six groups of data overlapped to some extent on the score plot (Figure 2). Obvious separations were observed for both the MV100 and MV500 groups, which clustered far from the other groups. This indicated a disturbing effect of VPA and HFD co-treatment on the metabolome of the rat. However, the ability to discriminate between other subgroups was poor. To achieve better discrimination, a submodel was calculated to further evaluate the metabolic similarities and differences among the groups. Thus, the three-principal-component PLS-DA scoring plot ($R^2X=0.550$, $R^2Y=0.565$, and $Q^2Y=0.332$, Figure 3) showed better clustering of the different groups. This observation indicated that VPA treatment and an HFD alone can induce a significant alteration in the serum metabolome and that cotreatment with VPA and HFD could aggravate changes in the serum metabolome.

Identification of relevant markers induced by VPA and HFD

Potentially relevant markers induced by VPA or HFD were identified by comparing the data between the control and the V100 (or V500) groups and the data between the model and the MV100 (or MV500) groups. Among the metabolites identified in this study, the analytes that contributed most to the induction of VPA and HFD were further confirmed by performing a one-way analysis of variance (ANOVA) with a significance level of $P<0.05$ (Supplementary Table S2–S4). The metabolites involved in conventional metabolic pathways (amino acid, lipid, and carbohydrate metabolism) were summarized.

In serum, the HFD and/or VPA treatment led to variation in the levels of endogenous metabolites. The levels of some ketogenic amino acids (eg, isoleucine, tryptophan), FFAs (eg, oleic acid, octadecanoic), 3-hydroxy-butanoic acid, and uric acid were markedly elevated, whereas docosahexaenoic acid, alpha-tocopherol, and myo-inositol-1-phosphate decreased following treatment with an HFD. In the VPA treatment groups, glycine, pyroglutamic acid, beta-alanine, sugar alcohols (eg, gluconic acid, glucuronic acid, and pentonic acid), and uric acid

increased, whereas oleic acid and cholesterol decreased (see Supplementary Table S2 and Figure S4). The metabolites identified in urine were markedly fewer than those in serum. Beta-alanine, thymidine, hippuric acid, 3-hydroxy-3-methylglutaric acid, and phosphoric acid decreased, whereas 3-hydroxy-butanonic acid and glyceric acid were up-regulated following the HFD. For the rats treated with VPA, we observed decreases in urea, hippuric acid, beta-alanine, thymidine, inositol, lactic acid, galactonic acid, and heptanoic acid, whereas gluturonic acid, glucuronic acid, lactose, and hexanedioic acid increased (Supplementary Table S3, and Figure S5).

Compared with serum and urine, bile metabolome may provide a more direct and immediate link to the pathological changes in the liver. The bile levels of glucogenic amino acids (eg, lysine, serine, threonine, ornithine, and alanine), lactic acid, gluconic acid, 3-hydroxy-butanonic acid, oleic acid, and urea increased; by contrast, the levels of glycine, pyroglutamic acid, and docosahexaenoic acid decreased in the groups fed an HFD (Supplementary Table S4 and Figure S6). It was surprising that we observed statistically significant decreases in almost all the amino acids detected, particularly glucogenic, ketogenic amino acids, citric acid, and free fatty acid classes in the VPA treatment groups. By contrast, the peak levels of sugar alcohols (eg, gluconic acid, glucuronic acid, gluturonic acid, and threonic acid) were sharply elevated in all the VPA treatment groups (Figure 4 and 5). In addition, most amino acids, citric acid and long-chain FFAs (eg, docosahexaenoic acid) were further decreased in VPA combined with HFD treatments (MV100 and MV500) compared with VPA mono-treatment groups. These showed the disrupting effects of an HFD and VPA on liver metabolism.

Discussion

VPA- and HFD-induced hepatotoxicity are both related to interference with the mitochondrial β -oxidation pathway^[41, 42]. However, very little is currently known about the interactions between HFD and VPA and the induction of hepatotoxicity. The current study contributed the novel observation that HFD

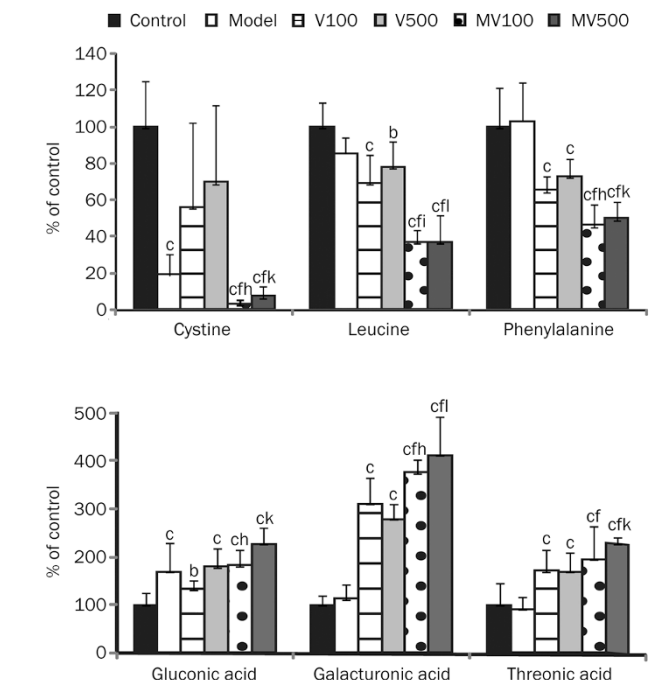


Figure 5. Major biomarkers detected from the bile metabolome. The data are shown as the mean \pm SD ($n=6$), normalized to the control group and expressed as a % of the control group. The statistical analysis was performed using an ANOVA, with values of $P<0.01$ or $P<0.05$ indicating significance. ^b $P<0.05$, ^c $P<0.01$ compared with the control group; ^f $P<0.01$ compared with the model group; ^h $P<0.05$ compared with the V100 group; ^k $P<0.05$, ^l $P<0.01$ compared with the V500 group. The control rats received only a standard diet; the model rats received only an HFD; V100, VPA, 100 mg \cdot kg⁻¹ \cdot d⁻¹, ig, and a standard diet; V500 group, VPA, 500 mg \cdot kg⁻¹ \cdot d⁻¹, ig, and a standard diet; MV100, VPA, 100 mg \cdot kg⁻¹ \cdot d⁻¹, ig, and an HFD; MV500, VPA, 500 mg \cdot kg⁻¹ \cdot d⁻¹, ig, and an HFD.

and VPA aggravated hepatic steatosis and hepatotoxicity, according to histopathological, biochemical, and metabolic studies.

In line with previous reports^[43–45], we found that both HFD

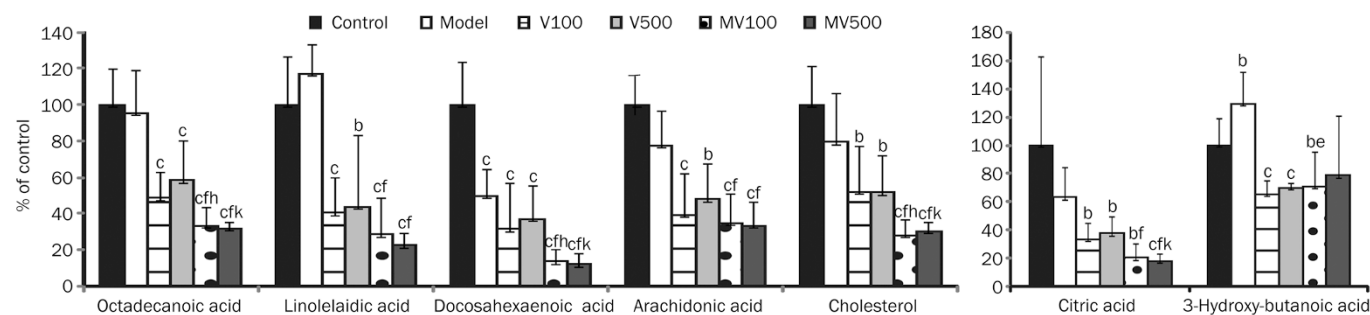


Figure 4. Major biomarkers detected from the bile metabolome. The data are shown as the mean \pm SD ($n=6$), normalized to the control group and expressed as a % of the control group. The statistical analysis was performed using an ANOVA, with values of $P<0.01$ or $P<0.05$ indicating significance. ^b $P<0.05$, ^c $P<0.01$, compared with the control group. ^e $P<0.05$, ^f $P<0.01$ compared with the model group. ^h $P<0.05$ compared with the V100 group. ^k $P<0.05$ compared with the V500 group. The control rats received only a standard diet; the model rats received only an HFD; V100, VPA, 100 mg \cdot kg⁻¹ \cdot d⁻¹, ig, and a standard diet; V500 group, VPA, 500 mg \cdot kg⁻¹ \cdot d⁻¹, ig, and a standard diet; MV100, VPA, 100 mg \cdot kg⁻¹ \cdot d⁻¹, ig, and an HFD; MV500, VPA, 500 mg \cdot kg⁻¹ \cdot d⁻¹, ig, and an HFD.

and VPA treatments resulted in significant elevations in the levels of lipids both in the plasma and liver. Co-treatment with an HFD and VPA provoked a more dramatic accumulation of lipids in the liver, which suggested a disruptive effect on hepatic lipid catabolism. LDL-c and HDL-c are synthesized in the hepatocyte and secreted into the plasma, and the dose-dependent decreases in the plasma levels of LDL-c and HDL-c in the VPA mono-treatment groups indicated hepatic dys-synthesis induced by VPA. The serum levels of ALT and AST did not change significantly, whereas the levels of MDA and α -GST increased significantly following VPA treatment for 8 weeks. This indicated that the plasma levels of both MDA and α -GST might reflect early alterations in hepatocellular integrity following the onset of drugs better than either ALT or AST and with a greater degree of sensitivity. The observations indicated that VPA could combine with an HFD to further disrupt hepatic lipid catabolism and the availability of hepatic lipids for energy generation. The net consequence could be more severe hepatic steatosis and hepatotoxicity.

To delineate the disturbance of endogenous metabolites and the potential underlying mechanisms of the interactive effect of HFD and VPA on disrupting liver metabolism, we performed a detailed metabolomic study of various biofluids, including serum, bile, and urine. Because bile metabolome is a direct and immediate indicator of liver function, we focus on the bile biomarkers in the discussion. When possible, the potential link between bile metabolites and those in serum and urine is also discussed, aiming to provide a systematic review of HFD/VPA-induced metabolome alterations. According to statistical measures, VPA treatment alone significantly decreased most FFAs, such as stearic acid (eg, octadecanoic acid), linoleic acid, oleic acid, docosahexaenoic acid, arachidonic acid, and cholesterol levels in the bile. Although the levels of most FFAs were less altered in the rat bile of the model group, a more dramatic decrease in these FFAs was observed in the HFD and VPA co-treatment groups (Figure 4), suggesting a combined effect of HFD and VPA in disrupting FFA metabolism.

TG is hydrolyzed to become glycerol and FFAs. FFAs are the most important energy source; they are mainly metabolized by intramitochondrial β -oxidation in the liver and muscles. Acetyl-CoA is generated via the β -oxidation route from FFAs. Some acetyl-CoA enters into the tricarboxylic acid (TCA) cycle for energy generation; some might be converted to ketone bodies, such as acetoacetate, 3-hydroxy butanoic acid and acetone. Several previous reports have shown that VPA and its intramitochondrial metabolites can sequester mitochondrial-free CoA, thereby inhibiting CoA-dependent metabolic processes^[42, 46, 47]. In previous study, the levels of TG, glycerol and FFAs in the plasma and the liver increased in a dose-dependent manner with VPA and increased further in response to the combination of VPA with an HFD, indicating that excessive fats accumulate *in vivo* after VPA and HFD treatments^[40]. On the contrary, citric acid, a key TCA intermediate, decreased in the bile after the VPA administration and even after the combined treatment with the HFD (Figure

4), which indicated that the availability of the TCA cycle for energy-dependent metabolism was decreased, thus resulting in a deficiency of adenosine triphosphate (ATP). The levels of biliary citric acid and biliary 3-hydroxy butanoic acid were significantly decreased in the VPA treatment groups. These observations suggest that VPA impairs the mitochondrial β -oxidation of FFAs, a reaction that could be aggravated with the combination of VPA and an HFD, thus enhancing the lipid accumulation in the hepatocytes and impeding substance metabolism.

Essential amino acids (EAAs, eg, lysine, tryptophan, phenylalanine, leucine, isoleucine, etc) cannot be synthesized *in vivo*, and the catabolism of amino acids mainly proceeds in the hepatocytes. In our study, it was surprising to observe that all the EAAs decreased significantly in the VPA treatment groups and decreased further in the treatments that combined VPA with an HFD (Supplementary Figure S6, Table S4). This result might also indicate an adaptive response of the hepatocytes: utilizing amino acids to produce ATP to compensate for the impaired metabolism of FFAs.

Because FFAs are mainly metabolized by CoA-dependent β -oxidation, the impairment of the mitochondria caused by VPA may increase the FFA accumulation in the hepatocytes and other metabolic pathways for FFAs may be enhanced to compensate. In addition to intramitochondrial β -oxidation, microsomal α and ω -oxidation are also pathways of FFA oxidation. The increase in ω -oxidation metabolites indicated an adaptive response of the hepatocytes from impaired mitochondrial oxidation to microsomal oxidation. Indeed, whereas 3-hydroxy butanoic acid significantly decreased in the bile and urine of the VPA treatment group, the ω -oxidation metabolites of FFAs, hexanedioic acid and heptanedioic acid were significantly elevated in the urine (Supplementary Figure S5). These findings strongly indicated that the β -oxidation of FFAs in the hepatocyte mitochondria was impaired by VPA. Furthermore, VPA counteracted the increase in 3-hydroxy-butanoic acid that was induced by the HFD. Thus, it could be suggested that an HFD provides more FFAs and that VPA inhibits the β -oxidation of FFAs. Consequently, an HFD and VPA may aggravate the abnormal accumulation of FFAs in the hepatocytes, resulting in liver injury.

Both urea and hippuric acid are primarily synthesized in liver mitochondria and depend on the concentration of ATP, which serves as a marker of hepatic mitochondria function^[48]. As shown in Figure 6 and Supplementary Figure S5, the levels of hippuric acid in the urine decreased after VPA administration and more dramatically after the combined treatment with an HFD, whereas the levels of its upstream metabolites, benzoic acid and glycine, increased in the VPA treatment groups. The same phenomenon was found for urea: the level of urea in the urine decreased in the VPA treatment groups while the precursor metabolites for urea synthesis, aspartic acid and ornithine, increased slightly (Supplementary Figure S5, Table S2 and S3). Moreover, the increased levels of urinary 3-hydroxy-3-methylglutaric acid (Figure 7) indicated the disruption of the final step in ketogenesis and leucine catabo-

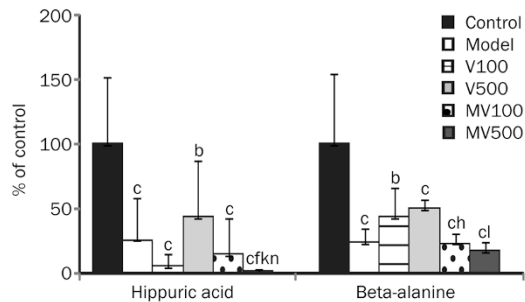


Figure 6. Major biomarkers detected from urine metabolome. The data are shown as the mean \pm SD ($n=6$), normalized to the control group and expressed as a % of the control group. The statistical analysis was performed using an ANOVA, with values of $P<0.01$ or $P<0.05$ indicating significance. ^b $P<0.05$, ^c $P<0.01$ compared with the control group; ^f $P<0.01$ compared with the model group; ^h $P<0.05$, the MV100 group compared with the V100 group. ^k $P<0.05$, ^l $P<0.01$, the MV500 group compared with the V500 group. ⁿ $P<0.05$, the MV500 group compared with the MV100 group. The control rats received only a standard diet; the model rats received only an HFD; V100, VPA, 100 mg $\text{kg}^{-1}\text{d}^{-1}$, ig, and a standard diet; V500 group, VPA, 500 mg $\text{kg}^{-1}\text{d}^{-1}$, ig, and a standard diet; MV100, VPA, 100 mg $\text{kg}^{-1}\text{d}^{-1}$, ig, and an HFD; MV500, VPA, 500 mg $\text{kg}^{-1}\text{d}^{-1}$, ig, and an HFD.

lism, which is catalyzed by the intramitochondrial enzyme 3-hydroxy-3-methylglutaryl-CoA lyase^[49, 50]. These observations further suggest that VPA may lead to mitochondrial dysfunction and impairment, which could be aggravated when combined with an HFD.

Overall, 70% of cholesterol is synthesized from acetyl-CoA in the hepatocytes. It is an integral component of all eukaryotic cell membranes and is essential for normal cellular function^[51, 52]. The decreased level of cholesterol both in the bile and in serum after VPA treatment further confirmed the deficiency of acetyl-CoA induced by VPA. Polyunsaturated fatty acids (PFAs, *eg*, linoleic acid, oleic acid, docosahexaenoic acid, arachidonic acid) are essential *in vivo* because they cannot be synthesized by humans. In contrast to the decrease in bile FFAs, a dramatic accumulation of FFAs in the liver was observed in the VPA treatment groups. It is known that FFAs and cholesterol are secreted across the apical (canalicular) membrane of the hepatocytes by ATP-binding transmembrane transporters^[53]. The elevated hepatic but reduced biliary FFAs indicate compromised FFA transport machinery, which could be due to the reduced expression of transporters and/or the energy (ATP) induced by VPA. Taken together, the metabolomic analyses of the biomarkers involved in FFA and amino acid metabolism strongly suggest that VPA in combination with an HFD impairs the mitochondrial function of the hepatocytes, leading to the hepatic accumulation of FFAs that may aggravate liver injuries and hepatic steatosis.

In addition to the hepatic β -oxidation of FFAs, muscle is another important organ responsible for FFA β -oxidation. In contrast to the lower levels of intermediate TCA in bile, the intermediates of TCA in serum increased after the VPA treatments (Supplementary Figure S4). The gross anatomy of the

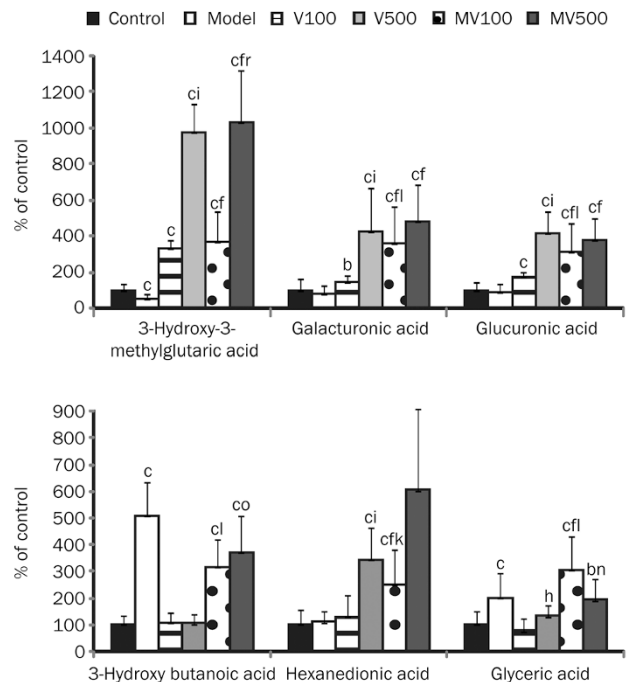


Figure 7. Major biomarkers detected from the urine metabolome. The data are shown as the mean \pm SD ($n=6$), normalized to the control group and expressed as a % of the control group. The statistical analysis was performed using an ANOVA, with values of $P<0.01$ or $P<0.05$ indicating significance. ^b $P<0.05$, ^c $P<0.01$ compared with the control group. ^f $P<0.05$, ^f $P<0.01$ compared with the model group. ^h $P<0.05$, ^l $P<0.01$, the V500 group compared with the V100 group. ^k $P<0.05$, ^l $P<0.01$, the MV100 group compared with the V100 group. ⁿ $P<0.05$, ^o $P<0.01$, the MV500 group compared with the V500 group. ^r $P<0.01$, the MV500 group compared with the MV100 group. The control rats received only a standard diet; the model rats received only an HFD; V100, VPA, 100 mg $\text{kg}^{-1}\text{d}^{-1}$, ig, and a standard diet; V500 group, VPA, 500 mg $\text{kg}^{-1}\text{d}^{-1}$, ig, and a standard diet; MV100, VPA, 100 mg $\text{kg}^{-1}\text{d}^{-1}$, ig, and an HFD; MV500, VPA, 500 mg $\text{kg}^{-1}\text{d}^{-1}$, ig, and an HFD.

animal showed visceral fat accumulation while the limbs were emaciated, further certifying that the β -oxidation of FFAs in extrahepatic areas compensated for the impaired metabolism of FFAs in the liver.

It was notable that VPA significantly elevated the level of glucuronic acid in the bile, urine, and serum (Figure 5 and 7). Glucuronic acid is the donor of UDP-glucuronyltransferase, which conjugates both endogenous and exogenous toxicants^[54, 55]. Because VPA itself is mainly metabolized by glucuronidation and mitochondrial β -oxidation, an increase in glucuronic acid may represent a compensatory mechanism by the hepatocytes to ameliorate VPA-induced hepatotoxicity. The underlying mechanism and its significance warrants further investigation.

Conclusion

The present study improves our understanding of the conceptual framework for the potential mechanisms of the drug/diet interaction in hepatotoxicity. VPA predominantly impairs the

β -oxidation of FFAs and thus provokes hepatic accumulation of FFAs. In addition, an HFD could aggravate the effects that were stimulated by VPA. These observations collectively indicate that VPA and an HFD induce more severe hepatic steatosis and hepatotoxicity when they are concomitant. Our findings strongly indicate that patients undergoing VPA therapy in a clinical setting should avoid long-term consumption of an HFD. Moreover, patients who have received VPA therapy should be very carefully monitored in an attempt to prevent asymptomatic hepatic steatosis and hepatotoxicity.

Acknowledgements

This study was supported by the National Natural Science Foundation of China (Grants 81072695 and 91029746), the National Basic Research Program of China ("973 Program") (Grant 2011CB505300-03), the Foundation for the Author of National Excellent Doctoral Dissertation of China (Grant 200979); the Natural Science Foundation of Jiangsu Province (Grant BK2010066), and the Program for a New Century Excellent Talent in University (Grant NCET-09-0770).

Author contribution

Li-fang ZHANG, Hai-ping HAO, Guang-ji WANG, and Ji-ye A designed the research; Li-fang ZHANG, Ling-sheng LIU, Xiao-man CHU, Hao XIE, Cen GUO, Meng-jie LI, and Li-juan CAO performed the experiments; Li-fang ZHANG, Ling-sheng LIU, Hao XIE, and Bei CAO analyzed the data; and Li-fang ZHANG, Hai-ping HAO, and Ji-ye A wrote the paper.

Supplementary information

Supplemental Tables and Figures are available at the website of *Acta Pharmacologica Sinica*.

References

- 1 Simon D, Penry JK. Sodium Di-N-propylacetate (DPA) in the treatment of epilepsy. *Epilepsia* 1975; 16: 549–73.
- 2 Chapman A, Keane PE, Meldrum BS, Simiand J, Vernieres JC. Mechanism of anticonvulsant action of valproate. *Prog Neurobiol* 1982; 19: 315–59.
- 3 Chavez-Blanco A, Segura-Pacheco B, Perez-Cardenas E, Taja-Chayeb L, Cetina L, Candelaria M. Histone acetylation and histone deacetylase activity of magnesium valproate in tumor and peripheral blood of patients with cervical cancer. A phase I study. *Mol Cancer* 2005; 4: 22.
- 4 Goodyear O, Agathangelou A, Novitzky-Basso I, Siddique S, McSkeane T, Ryan G, et al. Induction of a CD8⁺ T-cell response to the MAGE cancer testis antigen by combined treatment with azacitidine and sodium valproate in patients with acute myeloid leukemia and myelodysplasia. *Blood* 2010; 116: 1908–18.
- 5 Eadie MJ, Hooper WD, Dickinson RG. Valproate-associated hepatotoxicity and its biochemical mechanisms. *Med Toxicol Adverse Drug Exp* 1988; 3: 85–106.
- 6 Tong V, Teng XW, Chang TK, Abbott FS. Valproic acid I: time course of lipid peroxidation biomarkers, liver toxicity, and valproic acid metabolite levels in rats. *Toxicol Sci* 2005; 86: 427–35.
- 7 Luef GJ, Waldmann M, Sturm W, Naser A, Trinkka E, Unterberger I, et al. Valproate therapy and nonalcoholic fatty liver disease. *Ann Neurol* 2004; 55: 729–32.
- 8 Becker CM, Harris RA. Influence of valproic acid on hepatic carbohydrate and lipid metabolism. *Arch Biochem Biophys* 1983; 223: 381–92.
- 9 CoudéFX, Grimber G, Pelet A, Benoit Y. Action of the antiepileptic drug, valproic acid, on fatty acid oxidation in isolated rat hepatocytes. *Biochem Biophys Res Commun* 1983; 115: 730–6.
- 10 Pessayre D, Mansouri A, Haouzi D, Fromenty B. Hepatotoxicity due to mitochondrial dysfunction. *Cell Biol Toxicol* 1999; 15: 367–73.
- 11 Knapp AC, Todesco L, Beier K, Terracciano L, Sägeser H, Reichen J, et al. Toxicity of valproic acid in mice with decreased plasma and tissue carnitine stores. *J Pharmacol Exp Ther* 2008; 324: 568–75.
- 12 Oguma T, Yamada H, Sawaki M, Narita N. Pharmacokinetic analysis of the effects of different foods on absorption of cefaclor. *Antimicrob Agents Chemother* 1991; 35: 1729–35.
- 13 OSullivan A, Gibney MJ, Brennan L. Dietary intake patterns are reflected in metabolomic profiles: potential role in dietary assessment studies. *Am J Clin Nutr* 2011; 93: 314–21.
- 14 Bellentani S, Saccoccio G, Masutti F, Crocè LS, Brandi G, Sasso F. Prevalence and risk factors for hepatic steatosis in northern Italy. *Ann Intern Med* 2002; 132: 112–7.
- 15 de Alwis NM, Day CP. Non-alcoholic fatty liver disease: the mist gradually clears. *J Hepatol* 2008; 48: S104–12.
- 16 Satia-Abouta J, Patterson RE, Schiller RN, Kristal AR. Energy from fat is associated with obesity in US men: results from the Prostate Cancer Prevention Trial. *Prev Med* 2002; 34: 493–501.
- 17 Fan JG, Farrell GC. Epidemiology of non-alcoholic fatty liver disease in China. *J Hepatol* 2009; 50: 204–10.
- 18 Angulo P. Nonalcoholic fatty liver disease. *N Engl J Med* 2002; 346: 1221–31.
- 19 Li H, Xie Z, Lin J, Song H, Wang Q, Wang K, et al. Transcriptomic and metabolomic profiling of obesity-prone and obesity-resistant rats under high fat diet. *J Proteome Res* 2011; 7: 4775–83.
- 20 Rector RS, Thyfault JP, Uptergrove GM, Morris EM, Naples SP, Borengasser SJ, et al. Mitochondrial dysfunction precedes insulin resistance and hepatic steatosis and contributes to the natural history of non-alcoholic fatty liver disease in an obese rodent model. *J Hepatol* 2010; 52: 727–36.
- 21 Verrotti A, Agostinelli S, Parisi P, Chiarelli F, Coppola G. Nonalcoholic fatty liver disease in adolescents receiving valproic acid. *Epilepsy Behav* 2011; 20: 382–5.
- 22 Nicholson JK, Lindon JC, Holmes E. 'Metabonomics': understanding the metabolic responses of living systems to pathophysiological stimuli via multivariate statistical analysis of biological NMR spectroscopic data. *Xenobiotica* 1999; 29: 1181–9.
- 23 Nicholson JK, Connelly J, Lindon JC, Holmes E. Metabonomics: a platform for studying drug toxicity and gene function. *Nat Rev Drug Discov* 2002; 1: 153–61.
- 24 Gu SH, A JY, Wang GJ, Zha WB, Yan B, Zhang Y, et al. Metabolomic profiling of liver metabolites by gas chromatography-mass spectrometry and its application to characterizing hyperlipidemia. *Biomed Chromatogr* 2010; 24: 245–52.
- 25 Schnackenberg LK, Jones RC, Thyparambil S, Taylor JT, Han T, Tong W, et al. An integrated study of acute effects of valproic acid in the liver using metabolomics, proteomics, and transcriptomics platforms. *OMICS* 2006; 10: 1–14.
- 26 Barr J, Vazquez-Chantada M, Alonso C, Perez-Cormenzana M, Mayo R, Galán A, et al. Liquid chromatography-mass spectrometry-based parallel metabolic profiling of human and mouse model serum reveals putative biomarkers associated with the progression of nonalcoholic fatty liver disease. *J Proteome Res* 2010; 9: 4501–12.
- 27 Lee MH, Hong I, Kim M, Lee BH, Kim JH, Kang KS, et al. Gene expres-

- sion profiles of murine fatty liver induced by the administration of valproic acid. *Toxicol Appl Pharmacol* 2007; 220: 45–59.
- 28 Perucca E. Pharmacological and therapeutic properties of valproate: a summary after 35 years of clinical experience. *CNS Drugs* 2002; 16: 695–714.
- 29 Lee MH, Kim M, Lee BH, Kim JH, Kang KS, Kim HL, et al. Subchronic effects of valproic acid on gene expression profiles for lipid metabolism in mouse liver. *Toxicol Appl Pharmacol* 2008; 226: 271–84.
- 30 Hakk H, Larsen G, Bergman A, Orn U. Metabolism, excretion and distribution of the flame retardant tetrabromobisphenol-A in conventional and bile-duct cannulated rats. *Xenobiotica* 2000; 30: 881–90.
- 31 Bachir-Cherif D, Blum D, Braendli-Baiocco A, Chaput E, Pacheco GC, Flint N, et al. Characterization of post-surgical alterations in the bile duct-cannulated rat. *Xenobiotica* 2011; 41: 701–11.
- 32 A JY, Hang Q, Wang GJ, Zha WB, Yan B, Ren H, et al. Global analysis of metabolites in rat and human urine based on gas chromatography/time-of-flight mass spectrometry. *Anal Biochem* 2008; 379: 20–6.
- 33 Liu LS, A JY, Wang GJ, Yan B, Zhang Y, Wang X, et al. Differences in metabolite profile between blood plasma and serum. *Anal Biochem* 2010; 406: 105–12.
- 34 Chen T, Xie G, Wang X, Fan J, Qiu Y, Zheng X, et al. Serum and urine metabolite profiling reveals potential biomarkers of human hepatocellular carcinoma. *Mol Cell Proteomics* 2011; 10: M110.004945.
- 35 A J, Trygg J, Gullberg J, Johansson AI, Jonsson P, Antti H, et al. Extraction and GC/MS analysis of the human blood plasma metabolome. *Anal Chem* 2005; 77: 8086–94.
- 36 Jonsson P, Johansson AI, Gullberg J, Trygg J, A JY, Grung B, et al. High-throughput data analysis for detecting and identifying differences between samples in GC/MS-based metabolomic analyses. *Anal Chem* 2005; 77: 5635–42.
- 37 Eriksson L, Johansson E, Kettaneh-Wold N. Multi- and megavariable data analysis principles and applications. 2001. Umetrics, Ume, Sweden.
- 38 Trygg J, Holmes E, Lundstedt T. Chemometrics in metabolomics. *J Proteome Res* 2007; 6: 469–79.
- 39 Eker C, Rydell R, Svanberg K, Andersson-Engels S. Multivariate analysis of laryngeal fluorescence spectra recorded *in vivo*. *Lasers Surg Med* 2001; 28: 259–66.
- 40 Zhang LF, Chu XM, Wang H, Xie H, Guo C, Cao LJ, et al. Dysregulations of UDP-glucuronosyltransferases in rats with valproic acid and high fat diet induced fatty liver. *Eur J Pharmacol* 2013; 721: 277–85.
- 41 Fromenty B, Pessayre D. Impaired mitochondrial function in microvesicular steatosis: effects of drugs, ethanol, hormones and cytokines. *J Hepatol* 1997; 26: 43–53.
- 42 Ponchault S, van Hoof F, Veitch K. *In vitro* effects of valproate and valproate metabolites on mitochondrial oxidations: relevance of CoA sequestration to the observed inhibitions. *Biochem Pharmacol* 1992; 43: 2435–42.
- 43 Silva MF, Ruiten JP, IJlst L, Jakobs C, Duran M, de Almeida IT, et al. Differential effect of valproate and its D2- and D4-unsaturated metabolites, on the β -oxidation rate of long-chain and medium-chain fatty acids. *Chem-Biol Interact* 2001; 137: 203–12.
- 44 Toye AA, Dumas ME, Blancher C, Rothwell AR, Fearnside JF, Wilder SP, et al. Subtle metabolic and liver gene transcriptional changes underlie diet-induced fatty liver susceptibility in insulin-resistant mice. *Diabetologia* 2007; 50: 1867–79.
- 45 Xie Z, Li H, Wang K, Lin J, Wang Q, Zhao G, et al. Analysis of transcriptome and metabolome profiles alterations in fatty liver induced by high-fat diet in rat. *Metabolism* 2010; 59: 54–60.
- 46 Becker CM, Harris RA. Influence of valproic acid on hepatic carbohydrate and lipid metabolism. *Arch Biochem Biophys* 1983; 223: 381–92.
- 47 Pourahmad J, Eskandari MR, Kaghazi A, Shaki F, Shahraki J, Fard JK. A new approach on valproic acid induced hepatotoxicity: involvement of lysosomal membrane leakiness and cellular proteolysis. *Toxicol In Vitro* 2012; 26: 545–51.
- 48 Krähenbühl L, Reichen J, Talos C, Krähenbühl S. Benzoic acid metabolism reflects hepatic mitochondrial function in rats with long-term extrahepatic cholestasis. *Hepatology* 1997; 25: 278–83.
- 49 Pie J, Casals N, Puisac B, Hegardt FG. Molecular basis of 3-hydroxy-3-methylglutaric aciduria. *J Physiol Biochem* 2003; 59: 311–21.
- 50 Koling S, Kalhoff H, Schauerer P, Lehnert W, Diekmann L. 3-hydroxy-3-methylglutaric aciduria (case report of a female Turkish sisters with 3-hydroxy-3-methylglutaryl-Coenzyme A lyase deficiency. *Klin Padiatr* 2000; 212: 113–6.
- 51 Batetta B, Sanna F. Cholesterol metabolism during cell growth: Which role for the plasma membrane? *Eur J Lipid Sci Technol* 2006; 108: 687–99.
- 52 Sviridov D, Nestel P. Dynamics of reverse cholesterol transport: Protection against atherosclerosis. *Atherosclerosis* 2002; 161: 245–54.
- 53 Esteller A. Physiology of bile secretion. *World J Gastroenterol* 2008; 14: 5641–9.
- 54 Kolodziejczyk J, Saluk-Juszczak J, Wachowicz B. *In vitro* study of the antioxidative properties of the glucose derivatives against oxidation of plasma components. *J Physiol Biochem* 2011; 67: 175–83.
- 55 Mak IT, Komarov AM, Kramer JH, Weglicki WB. Protective mechanisms of Mg-gluconate against oxidative endothelial cytotoxicity. *Cell Mol Biol* 2000; 46: 1337–44.